Journal of
Mechanics of
Materials and Structures

**BUCKLING AND NONLINEAR RESPONSE OF SANDWICH
PANELS WITH A COMPLIANT CORE AND
TEMPERATURE-DEPENDENT MECHANICAL PROPERTIES**

Yeoshua Frostig and Ole Thybo Thomsen

BUCKLING AND NONLINEAR RESPONSE OF SANDWICH PANELS WITH A COMPLIANT CORE AND TEMPERATURE-DEPENDENT MECHANICAL PROPERTIES

YEOSHUA FROSTIG AND OLE THYBO THOMSEN

This paper deals with the buckling response and nonlinear behavior of sandwich panels with *soft* cores that have temperature-dependent mechanical properties and are subjected to thermally induced deformations and mechanical loads simultaneously. This study investigates the effects of the degradation of properties of the core as a result of rising temperature on the response of the sandwich panel. Analyses are carried out for cases of pure thermal loading, with either uniform or gradient temperature fields through the depth of the panel, as well as for thermal loading acting simultaneously with external mechanical loads. The formulation is based on variational principles along with the high-order sandwich panel approach. It takes into account the flexibility of the core in the vertical direction as well as the dependency of the mechanical core properties of the temperature distribution through the core depth. The stress and deformation fields of the core have been solved *analytically*, including the case where the temperature-dependent properties attain a complex pattern. The buckling equations are derived using the perturbation technique, yielding a set of nonlinear algebraic equations for the case of a simply-supported panel and a uniform temperature field. The critical temperatures and modes of wrinkling and global buckling are determined numerically for some foam types of core made by Rohacell and Divinycell. The nonlinear response caused by thermally induced deformations is presented for Divinycell foam core with different temperature distributions through the depth of the core. Finally, the nonlinear response caused by the simultaneous action of external mechanical loading and increased temperatures on the compressive or the tensile side of the panel, with a thermal gradient through the core depth, is presented. The interaction between elevated temperatures and mechanical loads changes the response from a linear into an unstable nonlinear one when the degradation of the mechanical properties due to temperature changes is considered and the panel is unrestrained. Moreover, the unstable nonlinear behavior becomes even more severe when the face, loaded in compression, is subjected to elevated temperatures. This study reveals that a reliable, realistic design of a sandwich panel that is subjected to elevated temperature (within working temperature range) and mechanical loads must take into account the degradation of the properties of the core as a result of the thermal field even at working temperature range, especially when cores made of foam are considered.

1. Introduction

Modern structural sandwich panels are used for a variety of applications in most major industries. They usually consist of two face sheets made of either metal or composite laminated materials that are separated and bonded to a low-strength compliant core material. The use of sandwich structures is on the increase as primary and secondary structural components due to their superior qualities in terms of high strength to weight and stiffness to weight ratios, ease of manufacturing, acoustic and thermal insulation, and flexibility in design. Sandwich structures are often subjected to aggressive service conditions including external mechanical loads and elevated temperatures, which lead to thermally induced deformation loads and degradation of the material properties. Thermally induced deformations with and without external mechanical loads are in general associated with bending, buckling and a nonlinear response of the sandwich panel, with and without degradation of the material properties.

In general, the material properties of the constituents of a sandwich panel depend on the temperature field imposed on the structure. However, this dependency is usually ignored, even for cases where temperature fields are induced and the material properties degrade significantly with increasing temperatures. In many modern sandwich panel applications, the core material is made from polymer foam where significant changes in the properties may occur in the operating range of temperatures for the structure. For example, a Rohacell type of foam looses its heat distortion resistance at about 200° C [Rohacell 2004], while Divinycell foam loses its strength at about 80–100° C [Diab Group 2003; 2005 (private communication)]. Hence, it becomes extremely important to understand how the thermally induced degradation of the core properties lead to deformation loads, and large deformations affect the buckling and the nonlinear response of the sandwich panel with soft cores made of polymer foam. The response of a sandwich panel when subjected to an external mechanical load may involve a stable type of nonlinear response (such as a plate type of buckling response), or an unstable response (like the buckling response of a beam or a shell), and it depends on the sandwich panel layout, the geometrical and mechanical properties of the sandwich constituents, and the boundary conditions.

Moreover, when external mechanical loads act simultaneously with thermal loads (rising temperatures), the degradation of the material properties with rising temperature may shift the response from a linear and stable one into an unstable one. One of the objectives of this investigation is to study this occurrence.

Sandwich panels with vertically rigid cores made of metallic or polymer honeycombs have been considered by many researchers. It is usually assumed that the core is an *antiplane* and is incompressible (see [Plantema 1966; Allen 1969; Zenkert 1995; Vinson 1999]). Usually, the models adopted for predicting the linear and nonlinear load-response of sandwich panels are based on the *equivalent single layer* approach (ESL), where the layered panel (beam, plate or shell type) is replaced by an equivalent single layer with homogenized (equivalent) mechanical properties (see Mindlin first-order theory [Mindlin 1951]), and Reddy's high-order theories [Reddy 1984]. Recently Huang and Kardomateas [2002] and Kardomateas and Huang [2003] have used the ESL approach to analyze a sandwich panel with very large deformations. The classical and ESL computation models usually disregard the changes in the height of the core (the compressibility) when the panel is deformed.

Thermal buckling and nonlinear analyses using the ESL approach and using mechanical properties that are *independent* of temperature have been considered by a few authors: Ko [1994] treated the buckling

problem with various boundary conditions; Kant and S. [2000] used a first-order shear model along with finite element analysis for skew plates; Tessler et al. [2001] used a first-order shear deformable (FOSD) model along with a second–order polynomial for the vertical deflection; and Liew et al. [2004] used a FOSD model to investigate the effects of temperature dependent properties. Several researchers have used high-order models: these researchers include Najafizadeh and Heydari [2004], who adopted a third-order approach for the analysis of functionally graded material (FGM) circular plates; Kapuria and Achary [2004], who used a zig-zag third-order model for simply-supported panels; Shiau and Kuo [2004], who used a 72-DOF triangular finite element; and Matsunaga [2005], who used truncated power series expansions for representing the distribution of the displacements through the thickness of the panel (limited to simply-supported boundary conditions and buckling only).

Some research has been done on the response of panels with temperature-dependent mechanical properties. Chen and Chen [1989; 1991] used an FE solution to deal with buckling and postbuckling of a plate made of composite laminates with temperature-dependent mechanical properties. Gu and Asaro [2005] have analyzed a sandwich panel made of FGM face sheets and an incompressible core. They have used a power fitted function to describe the degradation of the mechanical properties due to rising temperature. Birman [2005] dealt with wrinkling of a simply-supported sandwich panel using the FOSD model, assuming material properties that are linearly dependent on temperature. Using the FOSD theory, Birman et al. [2006] and Liu et al. [2006] have considered the responses of a sandwich panel and a sandwich beam with temperature-dependent properties subjected to elevated temperatures. In general, the classical sandwich, described by ESL/FOSD and high-order computation models, mentioned above, disregards the changes in the height of the core (compressibility) during the deformation of the sandwich panel. Accordingly, they yield inaccurate results when used for sandwich panels with a soft/compliant core such as a polymer foam.

An approach that models the layered sandwich panel—that is, in being made of two face sheets and a core layer that are interconnected through fulfillment of equilibrium and compatibility conditions and in thus being able to incorporate the vertical flexibility of the core—represents a more consistent and rational approach and offers significant advantages when considering sandwich structures with compliant, soft cores. This approach has been implemented through a variational principle into the high-order sandwich panel theory approach (HSAPT), and has been successfully used for the analysis of various linear and nonlinear applications including hygrothermal effects [Frostig 1997]; buckling analysis of unidirectional sandwich panels [Frostig and Baruch 1993]; buckling analysis of sandwich plates [Frostig 1998]; nonlinear response to in-plane compressive loads [Sokolinsky and Frostig 2000]; and a general nonlinear response [Frostig et al. 2005]. Recently, Frostig and Thomsen [2007b] used the HSAPT approach to derive governing equations of the thermal buckling and the nonlinear response when taking into account the core thermal expansion in the vertical direction but with thermal independent properties. In a recently published paper, Frostig and Thomsen [2007a], have investigated numerically the thermal buckling and nonlinear response together with localized effects of a sandwich panel which has a compliant, soft core and temperature independent or averaged mechanical properties.

The literature survey reveals that most researchers generally ignore the effects associated with the vertical flexibility of the core. Moreover, they do not consider the nonlinear interaction response when the mechanical and the thermal loads are applied simultaneously, in which case the nonlinear interaction effects are enhanced when the mechanical properties are degrading as a result of their temperature

dependency. In such cases, the mechanical properties generally vary spatially (coordinates dependent), especially when temperature gradients through the depth of the sandwich panel are involved.

The present analysis incorporates the flexibility of the core in the vertical direction, the thermally induced deformations and mechanical loads, and the nonuniform core properties resulting from temperature dependency into the mathematical modeling according to the HSAPT approach. The variational principle of minimum of the total potential energy is used to derive the field equations along with the appropriate boundary conditions.

The formulation is based on the following *classical* assumptions for sandwich structures with compliant cores: the face sheets possess in-plane and bending rigidities; the face sheets and the core material are assumed be linear elastic; the face sheets undergo large displacements and moderate rotations (geometrically nonlinear); the core is considered as a two-dimensional linear elastic continuum with kinematic relations that correspond to small deformations (geometrically linear), where the core height may change during deformation, and section planes do not remain plane after deformation; the core possesses only shear and transverse normal stiffness, whereas the in-plane (longitudinal) normal stiffness is assumed to be nil; thermal fields are applied to the face sheets and the core with temperature dependent mechanical properties; full bond is assumed between the face sheets and the core; and the mechanical loads are applied to the face sheets only.

The paper briefly presents the nonlinear thermomechanical governing equations of the face sheets and the stress and displacement fields of the core. Temperature dependent material properties of the core are implemented into the governing equations through closed-form solutions of the governing core equations. The buckling equations are derived following the perturbation approach. Results of a numerical study investigating the effects of the temperature-dependent mechanical properties on the following are presented: buckling; nonlinear response due to thermal induced deformation only; and interaction response of thermal and mechanical loads. Finally a summary is presented and conclusions are drawn.

2. Nonlinear governing equations

The set of nonlinear governing equations used for the analysis herein have been derived through the minimization of the total potential energy following the procedure presented in [Frostig and Thomsen 2007a; 2007b]. The kinematic relations used for the isotropic face sheets, which are assumed to have temperature independent mechanical properties, correspond to large displacements with moderate rotations.

Thus, the nonlinear thermal field equations for the sandwich panel read:

$$-\left(\frac{d}{dx}N_{xxt}(x)\right) - \tau_{ct}(x)b_w - n_t = 0, \tag{1}$$

$$-N_{xxt}(x)\left(\frac{d^2}{dx^2}w_t(x)\right) - \left(\frac{d}{dx}N_{xxt}(x)\right)\left(\frac{d}{dx}w_t(x)\right) - \frac{1}{2}b_wd_t\left(\frac{d}{dx}\tau_{ct}(x)\right) - \left(\frac{d^2}{dx^2}M_{xxt}(x)\right)$$
$$-\sigma_{zzt}(x)b_w + \left(\frac{d}{dx}m_t(x)\right) - q_t = 0, \tag{2}$$

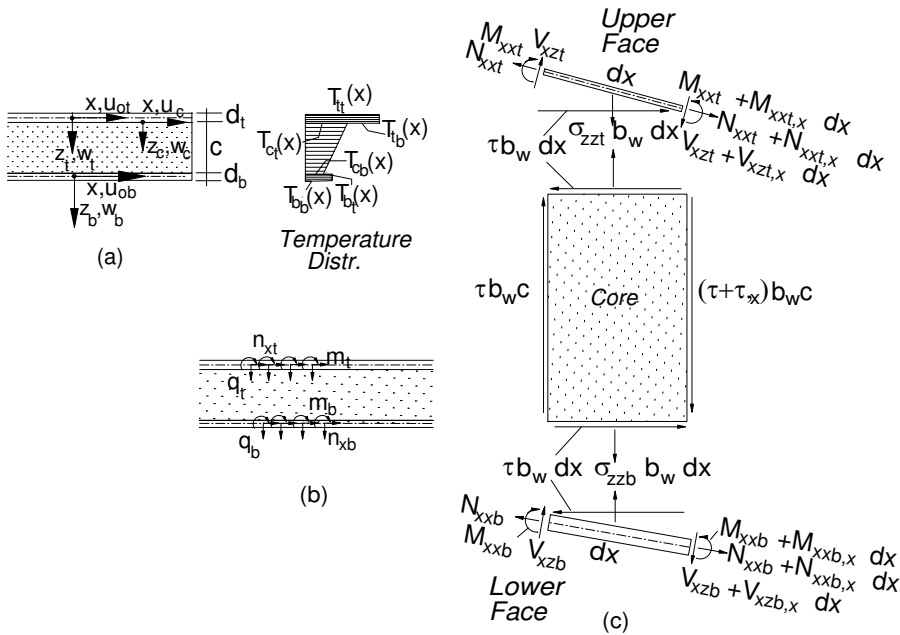$$-\left(\frac{d}{dx}N_{xxb}(x)\right) + \tau_{cb}(x)b_w - n_b = 0, \tag{3}$$

Figure 1. Geometry, loads, temperature distributions and internal stress resultants: (a) geometry, (b) external loads, (c) internal stress resultants and interfacial normal stresses.

$$-N_{xxb}(x)\left(\frac{d^2}{dx^2}w_b(x)\right) - \left(\frac{d}{dx}N_{xxb}(x)\right)\left(\frac{d}{dx}w_b(x)\right) - \frac{1}{2}b_w d_b\left(\frac{d}{dx}\tau_{cb}(x)\right) - \left(\frac{d^2}{dx^2}M_{xxb}(x)\right)$$
$$+ \sigma_{zzb}(x)b_w + \left(\frac{d}{dx}m_b(x)\right) - q_b = 0, \quad (4)$$

$$-\left(\frac{\partial}{\partial z_c}\tau_c(x, z_c)\right)b_w = 0, \qquad -\left(\frac{\partial}{\partial x}\tau_c(x, z_c)\right)b_w - \left(\frac{\partial}{\partial z_c}\sigma_{zz}(x, z_c)\right)b_w = 0, \qquad (5)$$

where N_{xxj} and M_{xxj} are the in-plane and bending moment stress resultants of each face sheet; $\tau_{cj}(x)$ and $\sigma_{zzj}(x)$ are the shear stresses and the vertical normal stresses at the face-core interfaces; n_j, q_j, and m_j are external distributed loads in the longitudinal and vertical direction and the bending moments exerted at the upper and the lower face sheets respectively; $w_j(x)$ are the vertical displacements of the upper and the lower face sheets; x is the longitudinal coordinate of the panel; b_w, d_j is the width of the panel and the thickness of the face sheets; $j = t, b$ denotes the upper or the lower face sheets; $\tau_c(x, z_c)$ and $\sigma_{zz}(x, z_c)$ are the shear and vertical normal stresses within the core; and z_c is vertical coordinate of the core. For sign conventions of coordinates, stresses, displacements, temperatures distribution, stress resultants, see Figure 1. The notation $(\ )_{,x}$ in Figure 1 refers to a derivative with respect to x.

The isotropic constitutive relations of the face sheets and the core yield the following additional load-displacement equations:

(i) For the face sheets (j=t,b):

$$N_{xxt}(x) - EA_j(x)\left(\left(\frac{d}{dx}u_{oj}(x)\right) + \frac{1}{2}\left(\frac{d}{dx}w_j(x)\right)^2\right) + EA_j(x)\alpha_j\left(\frac{1}{2}T_{j_t}(x) + \frac{1}{2}T_{j_b}(x)\right) = 0, \quad (6)$$

$$M_{xxj}(x) = EI_j\left(-\left(\frac{d^2}{dx^2}w_j(x)\right) - \frac{\alpha_j\left(T_{j_b}(x) - T_{j_j}(x)\right)}{d_j}\right). \quad (7)$$

(ii) For the core:

$$\frac{\sigma_{zz}(x, z_c)}{E_c(T_c(x, z_c))} = \left(\frac{\partial}{\partial z_c}w_c(x, z_c)\right) - \alpha_c T_c(x, z_c), \quad (8)$$

$$\frac{\tau_c(x, z_c)}{G_c(T_c(x, z_c))} = \left(\frac{\partial}{\partial z_c}u_c(x, z_c)\right) + \left(\frac{\partial}{\partial x}w_c(x, z_c)\right), \quad (9)$$

where $T_c(x, z_c)$ is the temperature distribution within the core that equals:

$$T_c(x, z_c) = T_{c_t}(x)\left(1 - \frac{z_c}{c}\right) + \frac{T_{c_b}(x)z_c}{c}, \quad (10)$$

and where the following refers to terms/quantities of the two face sheets: u_{oj} is the mid-plane in-plane displacements of the face sheets; EA_j and EI_j are the in-plane and flexural rigidities, respectively; α_j is the coefficient of thermal expansion of the face sheets; $T_{j_k}(x)$ $(k = t, b)$ are the temperatures at the upper and lower fibers of the faces, respectively. The terms/quantities related to the core include the following: $E_c(T_cx, z_c)$ and $G_c(T_cx, z_c)$ are the vertical modulus of elasticity and the shear modulus, respectively; $w_c(x, z_c)$ and $u_c(x, z_c)$ are the vertical and in-plane displacements, respectively; α_c is the coefficient of thermal expansion; $T_{c_k}(x, z_c)$ $(k = t, b)$ are the temperatures at the upper and lower fiber of the core, respectively; and c is the core height. See Figure 1 for sign conventions and temperature distributions.

The set of field equations, Equations (1) to (4), are given in an inexplicit form, since the face-core interfacial stresses are unknown. In addition, this set of equations does not fulfill the compatibility conditions of a full bond at the upper and the lower face-core interfaces.

The core stress fields using Equation (5) yields:

$$\tau_c(x, z_c) = \tau_{ct}(x) = \tau_{cb}(x) = \tau(x), \qquad \sigma_{zz}(x, z_c) = -\left(\frac{d}{dx}\tau(x)\right)z_c + \sigma_{zzt}(x). \quad (11)$$

Thus, the shear stresses within the core are uniform and the distribution of the vertical normal stresses through the depth of the core is linear. Hence, the vertical stress distribution and the displacements fields of the core are derived through the closed form solution of Equations (8) and (9). The compatibility conditions of the vertical displacement at the upper and the lower core-face interfaces and the compatibility condition of the longitudinal displacement at the upper interface are:

$$\sigma_{zzc}(x, z_c) = -E_{c1}(x, c)w_t(x) + E_{c1}(x, c)w_b(x) + \left(-z_c + \frac{E_{c1}(x, c)}{E_{c2}(x, c)}\right)\left(\frac{d}{dx}\tau(x)\right)$$

$$- \frac{1}{2}E_{c1}(x, c)\alpha_c T_{c_t}(x)c - \frac{1}{2}E_{c1}(x, c)c\alpha_c T_{c_b}(x); \quad (12)$$

$$w_c(x, z_c) = \left(\alpha_c z_c - \frac{1}{2}\frac{E_{c1}(x, c)\alpha_c c}{E_{c1}(x, z_c)} - \frac{1}{2}\frac{\alpha_c z_c^2}{c}\right)T_{c_t}(x) + \left(-\frac{1}{2}\frac{E_{c1}(x, c)\alpha_c c}{E_{c1}(x, z_c)} + \frac{1}{2}\frac{\alpha_c z_c^2}{c}\right)T_{c_b}(x)$$

$$+ \left(-\frac{E_{c1}(x, c)}{E_{c1}(x, z_c)} + 1\right)w_t(x) + \frac{E_{c1}(x, c)w_b(x)}{E_{c1}(x, z_c)} + \left(-\frac{1}{E_{c2}(x, z_c)} + \frac{E_{c1}(x, c)}{E_{c1}(x, z_c)E_{c2}(x, c)}\right)\left(\frac{d}{dx}\tau(x)\right);$$

(13)

$$u_c(x, z_c) = \left(\frac{1}{2}\frac{c\alpha_c\left(\frac{\partial}{\partial x}E_{c1}(x, c)\right)}{E_{c1z}(x, z_c)} - \frac{1}{2}\frac{E_{c1}(x, c)c\alpha_c\left(\frac{\partial}{\partial x}E_{c1z}(x, z_c)\right)}{E_{c1z}(x, z_c)^2}\right)T_{c_t}(x)$$

$$+ \left(\frac{1}{2}\frac{c\alpha_c\left(\frac{\partial}{\partial x}E_{c1}(x, c)\right)}{E_{c1z}(x, z_c)} - \frac{1}{2}\frac{E_{c1}(x, c)c\alpha_c\left(\frac{\partial}{\partial x}E_{c1z}(x, z_c)\right)}{E_{c1z}(x, z_c)^2}\right)T_{c_b}(x)$$

$$+ \left(\frac{\frac{\partial}{\partial x}E_{c1}(x, c)}{E_{c1z}(x, z_c)} - \frac{E_{c1}(x, c)\left(\frac{\partial}{\partial x}E_{c1z}(x, z_c)\right)}{E_{c1z}(x, z_c)^2}\right)w_t(x)$$

$$+ \left(-\frac{\frac{\partial}{\partial x}E_{c1}(x, c)}{E_{c1z}(x, z_c)} - \frac{E_{c1}(x, c)\left(\frac{\partial}{\partial x}E_{c1z}(x, z_c)\right)}{E_{c1z}(x, z_c)^2}\right)w_b(x)$$

$$+ \left(\frac{1}{2}\frac{E_{c1}(x, c)c\alpha_c}{E_{c1z}(x, z_c)} - \frac{1}{6}\frac{\alpha_c z_c^3}{c}\right)\left(\frac{d}{dx}T_{c_b}(x)\right)$$

$$+ \left(\frac{1}{2}\frac{E_{c1}(x, c)c\alpha_c}{E_{c1z}(x, z_c)} + \frac{1}{6}\frac{\alpha_c z_c^3}{c} - \frac{1}{2}\alpha_c z_c^2\right)\left(\frac{d}{dx}T_{c_t}(x)\right) + u_{ot}(x)$$

$$+ \left(\frac{E_{c1}(x, c)}{E_{c1z}(x, z_c)} - z_c - \frac{1}{2}d_t\right)\left(\frac{d}{dx}w_t(x)\right) - \frac{E_{c1}(x, c)\left(\frac{d}{dx}w_b(x)\right)}{E_{c1z}(x, z_c)} + \frac{\tau(x)}{G_{c1}(x, z_c)}$$

$$+ \left(-\frac{\frac{\partial}{\partial x}E_{c2z}(x, z_c)}{E_{c2z}(x, z_c)^2} + \frac{E_{c1}(x, c)\left(\frac{\partial}{\partial x}E_{c2}(x, c)\right)}{E_{c2}(x, c)^2 E_{c1z}(x, z_c)}\right.$$

$$\left. + \frac{E_{c1}(x, c)\left(\frac{\partial}{\partial x}E_{c1z}(x, z_c)\right)}{E_{c2}(x, c)E_{c1z}(x, z_c)^2} - \frac{\frac{\partial}{\partial x}E_{c1}(x, c)}{E_{c2}(x, c)E_{c1z}(x, z_c)}\right)\left(\frac{d}{dx}\tau(x)\right)$$

$$+ \left(-\frac{E_{c1}(x, c)}{E_{c2}(x, c)E_{c1z}(x, z_c)} + \frac{1}{E_{c2z}(x, z_c)}\right)\left(\frac{d^2}{dx^2}\tau(x)\right), \quad (14)$$

where

$$E_{c1}(x, c) = \cfrac{1}{\int\limits_0^c \cfrac{1}{E_c(T_c(x,z_c))} dz_c}, \qquad E_{c2}(x, c) = \cfrac{1}{\int\limits_0^c \cfrac{z_c}{E_c(T_c(x,z_c))} dz_c},$$

$$E_{c1}(x, z_c) = \cfrac{1}{\int\limits_0^{z_c} \cfrac{1}{E_c(T_c(x,z_1))} dz_1}, \qquad E_{c2}(x, z_c) = \cfrac{1}{\int\limits_0^{z_c} \cfrac{z_c}{E_c(T_c(x,z_1))} dz_1},$$

$$E_{c1z}(x, z_c) = \cfrac{1}{\int\limits_0^{z_c}\int\limits_0^{z_2} \cfrac{1}{E_c(T_c(x,z_1))} dz_1 dz_2}, \quad E_{c2z}(x, z_c) = \cfrac{1}{\int\limits_0^{z_c}\int\limits_0^{z_2} \cfrac{z_1}{E_c(T_c(x,z_1))} dz_1 dz_2},$$

$$G_{c1}(x, z_c) = \cfrac{1}{\int\limits_0^{z_c} \cfrac{1}{G_c(T_c(x,z_c))} dz_c}. \tag{15}$$

Hence, the interfacial vertical normal stresses at the upper and lower face-core interfaces (see Equations (2) and (4)) equal:

$$\sigma_{zzt}(x) = -E_{c1}(x, c)w_t(x) + E_{c1}(x, c)w_b(x) + \frac{E_{c1}(x, c)\left(\frac{d}{dx}\tau(x)\right)}{E_{c2}(x, c)} \tag{16}$$

$$-\frac{1}{2}E_{c1}(x, c)\alpha_c T_{c_t}(x)c - \frac{1}{2}E_{c1}(x, c)c\alpha_c T_{c_b}(x)$$

$$\sigma_{zzb}(x) = -E_{c1}(x, c)w_t(x) + E_{c1}(x, c)w_b(x) + \left(-c + \frac{E_{c1}(x, c)}{E_{c2}(x, c)}\right)\left(\frac{d}{dx}\tau(x)\right)$$

$$-\frac{1}{2}E_{c1}(x, c)\alpha_c T_{c_t}(x)c - \frac{1}{2}E_{c1}(x, c)c\alpha_c T_{c_b}(x).$$

The additional governing equation is the one that corresponds to the compatibility requirement in the longitudinal direction at the lower face-core interface, and it reads:

$$\left(-\frac{E_{c1}(x, c)}{E_{c1z}(x, z_c)} - \frac{1}{2}d_b\right)\left(\frac{d}{dx}w_b(x)\right) + \left(\frac{1}{2}\frac{c\alpha_c\left(\frac{\partial}{\partial x}E_{c1}(x, c)\right)}{E_{c1z}(x, z_c)} - \frac{1}{2}\frac{E_{c1}(x, c)c\alpha_c\left(\frac{\partial}{\partial x}E_{c1z}(x, z_c)\right)}{E_{c1z}(x, z_c)^2}\right)T_{c_t}(x)$$

$$+\left(\frac{1}{2}\frac{c\alpha_c\left(\frac{\partial}{\partial x}E_{c1}(x, c)\right)}{E_{c1z}(x, z_c)} - \frac{1}{2}\frac{E_{c1}(x, c)c\alpha_c\left(\frac{\partial}{\partial x}E_{c1z}(x, z_c)\right)}{E_{c1z}(x, z_c)^2}\right)T_{c_b}(x)$$

$$+\left(\frac{\frac{\partial}{\partial x}E_{c1}(x, c)}{E_{c1z}(x, z_c)} - \frac{E_{c1}(x, c)\left(\frac{\partial}{\partial x}E_{c1z}(x, z_c)\right)}{E_{c1z}(x, z_c)^2}\right)w_t(x)$$

$$+\left(-\frac{\frac{\partial}{\partial x}E_{c1}(x,c)}{E_{c1z}(x,z_c)}+\frac{E_{c1}(x,c)\left(\frac{\partial}{\partial x}E_{c1z}(x,z_c)\right)}{E_{c1z}(x,z_c)^2}\right)w_b(x)$$

$$+\left(\frac{1}{2}\frac{E_{c1}(x,c)c\alpha_c}{E_{c1z}(x,z_c)}-\frac{1}{6}\frac{\alpha_c z_c^3}{c}\right)\left(\frac{d}{dx}T_{c_b}(x)\right)+\left(\frac{1}{2}\frac{E_{c1}(x,c)c\alpha_c}{E_{c1z}(x,z_c)}+\frac{1}{6}\frac{\alpha_c z_c^3}{c}-\frac{1}{2}\alpha_c z_c^2\right)\left(\frac{d}{dx}T_{c_t}(x)\right)$$

$$+u_{ot}(x)+\left(\frac{E_{c1}(x,c)}{E_{c1z}(x,z_c)}-z_c-\frac{1}{2}d_t\right)\left(\frac{d}{dx}w_t(x)\right)-u_{ob}(x)+\frac{\tau(x)}{G_{c1}(x,z_c)}$$

$$+\left(-\frac{\frac{\partial}{\partial x}E_{c2z}(x,z_c)}{E_{c2z}(x,z_c)^2}+\frac{E_{c1}(x,c)\left(\frac{\partial}{\partial x}E_{c2}(x,c)\right)}{E_{c2}(x,c)^2E_{c1z}(x,z_c)}+\frac{E_{c1}(x,c)\left(\frac{\partial}{\partial x}E_{c1z}(x,z_c)\right)}{E_{c2}(x,c)E_{c1z}(x,z_c)^2}\right.$$

$$\left.-\frac{\frac{\partial}{\partial x}E_{c1}(x,c)}{E_{c2}(x,c)E_{c1z}(x,z_c)}\right)\left(\frac{d}{dx}\tau(x)\right)$$

$$+\left(-\frac{E_{c1}(x,c)}{E_{c2}(x,c)E_{c1z}(x,z_c)}+\frac{1}{E_{c2z}(x,z_c)}\right)\left(\frac{d^2}{dx^2}\tau(x)\right)=0,\quad(17)$$

where

$$E_{c1z}(x,z_c)=\frac{1}{\int_0^c\int_0^{z_2}\frac{1}{E_c(T_c(x,z_1))}dz_1dz_2},\qquad E_{c2z}(x,c)=\frac{1}{\int_0^c\int_0^{z_2}\frac{z_1}{E_c(T_c(x,z_1))}dz_1dz_2},$$

$$G_{c1}(x,c)=\frac{1}{\int_0^c\frac{1}{G_c(T_c(x,z_c))}dz_c}.\qquad(18)$$

Hence, the thermomechanical nonlinear governing set of equations are derived by substitution of the force-displacements equations, Equations (6) to (9), into the four field equations, Equations (1) to (4), and the fifth equation is the compatibility condition expressed by Equation (17). This set of equations corresponds to five unknowns: the longitudinal and vertical displacement of the upper and the lower face sheets and the shear stress in the core.

The boundary and the continuity conditions are based on fourteen unknown functions and are not presented herein for brevity. For details see [Frostig 1997].

3. Buckling analysis

The buckling analysis is based on the perturbation approach in which the nonlinear governing equations are linearized [Simitses 1976]. The linearized governing equations for the prebuckling and buckling stages appear in [Frostig and Thomsen 2007b] for a sandwich panel with *temperature-independent* mechanical properties and a uniform temperature field through the length and through the height of the panel.

For the case of a sandwich panel with *temperature-dependent* properties subjected to a longitudinally and vertically uniform temperature field, the critical temperatures (the wrinkling and global buckling modes) have been derived assuming the prebuckling case following the perturbation procedure described in [Frostig and Baruch 1993] and [Frostig and Thomsen 2007b]. In this procedure the thermal strain of the core in the vertical direction is ignored, which yields a membrane thermal prebuckling stage where the face sheets are subjected to in-plane stress resultants only due to the in-plane constraints imposed at the edges of the face sheets. The critical temperatures are determined through the closed-form solution of the buckling equations of a simply-supported panel that yields a set of algebraic equations. For this case it, is assumed that the two face sheets are of identical geometry and have temperature-independent mechanical properties that are uniform through the length of the panel. In addition, it is assumed that the core has uniform mechanical properties that depend on the temperature.

For the wrinkling mode where the two face sheets move in opposite directions (symmetric mode with respect to mid-height), the solution reads:

$$-\frac{2b_w E_c(T_{cr,wr})L^4 + EI_t m^4 \pi^4 c}{L^2 m^2 \pi^2 c} = -EA_t \alpha_t T_{cr,wr}, \quad (19)$$

where the critical half wave number m equals:

$$m = \text{integer}\left(\frac{2^{(1/4)}(b_w E_c(T_{cr,wr})EI_t^3 c^3)^{(1/4)} L}{EI_t \pi c}\right), \quad (20)$$

and where L is the length of the panel and $T_{cr,wr}$ is the critical temperature that yields a wrinkling buckling mode.

For the global buckling mode, where the two face sheets move in the same direction and with the same displacement value (a symmetric mode), the closed-form solution reads:

$$m^2 \pi^2 \Big(c^3 EA_t EI_t G_c(T_{cr,gl})\pi^4 m^4 + 6b_w EA_t E_c(T_{cr,gl})G_c(T_{cr,gl})L^4 c^2$$
$$+12cL^4 b_w EA_t d_t E_c(T_{cr,gl})G_c(T_{cr,gl}) + 12cEA_t EI_t E_c(T_{cr,gl})\pi^2 m^2 L^2$$
$$+24b_w EI_t E_c(T_{cr,gl})G_c(T_{cr,gl})L^4$$
$$+6L^4 b_w EA_t d_t^2 E_c(T_{cr,gl})G_c(T_{cr,gl})\Big) \Big/ \Big(L^2\big(12m^2\pi^2 L^2 cEA_t E_c(T_{cr,gl})$$
$$+m^4\pi^4 c^3 EA_t G_c(T_{cr,gl}) + 24b_w L^4 E_c(T_{cr,gl})G_c(T_{cr,gl})\big)\Big) = EA_t \alpha_t T_{cr,gl}, \quad (21)$$

where m is the critical half wave number and $T_{cr,gl}$ is the critical temperature, which corresponds to $m = 1$.

It should be noticed that, as a result of the temperature dependency, the critical temperatures can be evaluated only through the solution of the nonlinear algebraic equations, while for the case where the properties are temperature-independent, the critical values can be derived in terms of closed-form expressions [Frostig and Thomsen 2007b].

A numerical study, presented in the forthcoming section, has been conducted in order to determine the effects of the temperature-dependent properties of the core on the critical temperatures for the case of Rohacell WF and Divinycell P- and HP-types of foams. Figure 2 describes the nondimensional elastic
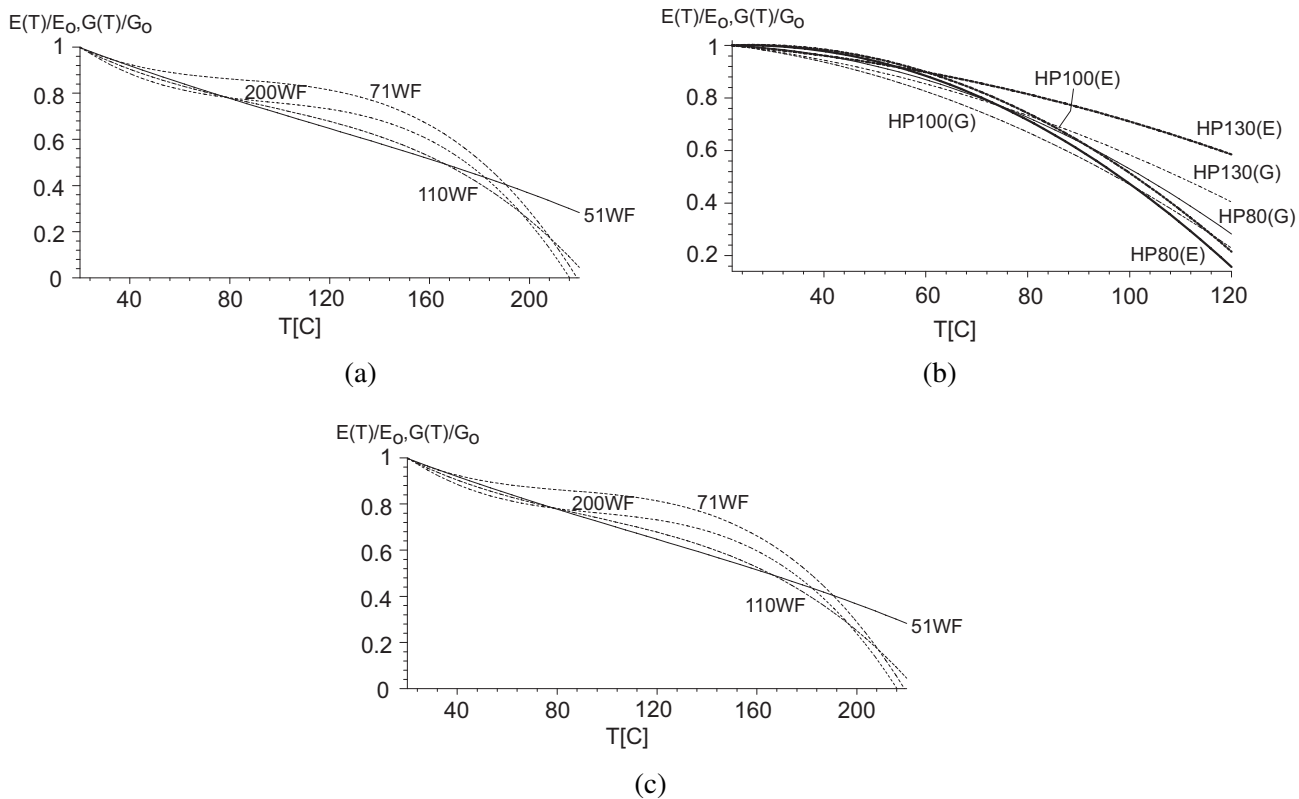
Figure 2. Normalized temperature-dependent elastic and shear moduli of various polymer foam cores: (a) Rohacell WF foam, (b) Divinycell HP foam, (c) Divinycell P foam. Legend: (E) – modulus of elasticity (thick lines), (G) – Shear modulus (dashed thin lines).

and shear moduli of these materials as functions of temperature. The curve fitted data appearing in Figure 2 are based on the data that appear in [Rohacell 2004] and [Diab Group 2005]. For the case of the Rohacell foam it is assumed that the degradation of the elastic and the shear moduli is the same (see Figure 2a). For the two Divinycell foams the degradation is slightly different for the elastic and the shear moduli, and it is denoted by the letters E and G in Figures 2b and Figure 2c.

The critical temperatures have been determined for foams with temperature independent and dependent mechanical properties for comparison (see Tables 1 and 2 for the different core materials). A sandwich beam with length of 1000 mm, width 30 mm, two aluminum face sheets of 0.5 mm thickness, CTE of 1e-5, modulus of elasticity of 69130 MPa, and a core height of 25 mm is investigated. The results in Tables 1 and 2 include the critical temperature for the wrinkling and the global buckling modes, as well as the value of the mechanical properties when the critical temperature values are reached.

The results for the WF foam made by Rohacell (see Table 1), reveal that when the E- and G-moduli at room temperature are considered and denoted as temperature independent properties (TI), the critical temperatures are much above the range of operating temperatures for this material. However, when the

Foam	Buckling-Properties Types	$T_{cr}{}^o$ [C]*	Mode Number (m)	$E_c(T_{cr})$ [MPa]	$G_c(T_{cr})$ [MPa]
51WF	Wr-TI**	384.7	97	70.5	22.1
	Wr-TD	201.7	70	21.1	6.6
	Gl-TI	136.2	1	70.5	22.1
	Gl-TD	122.5	1	44.0	13.8
71WF	Wr-TI	457.5	105	100.3	38.8
	Wr-TD	188.5	68	18.4	7.1
	Gl-TI	145.7	1	100.3	38.8
	Gl-TD	139.2	1	72.3	27.9
110WF	Wr-TI	601.5	121	169.5	63.3
	Wr-TD	194.7	69	19.7	7.3
	Gl-TI	151.2	1	169.5	63.3
	Gl-TD	143.1	1	95.5	35.6
200WF	Wr-TI	719.8	132	237.6	132.7
	Wr-TD	191.7	68	19.05	10.6
	Gl-TI	156.0	1	237.6	132.7
	Gl-TD	152.1	1	139.3	77.8

Table 1. Critical temperatures of Rohacell WF foam. Legend: Wr – wrinkling mode; Gl – global mode; TI – temperature-independent properties; TD – temperature-dependent properties. * With respect to an unheated panel at room temperature (20° C). ** Modulus of elasticity and shear modulus at room temperature.

temperature dependence of the E- and G-moduli of the core is included in the analyses (denoted by TD for *temperature-dependent* in Table 1), the predicted critical temperatures reach the upper range of the operating temperature of the foam, which is associated with very low values of E and G. Notice that for the case of wrinkling buckling mode, the half wave number is significantly reduced compared to the TI case. For most of the cases, the critical buckling mode is associated with global buckling.

Considering the results obtained for the Divinycell foams (see Table 2), similar trends are observed. The differences in the critical temperatures between the TI and the TD cases are significant, especially when the wrinkling buckling mode occurs. The differences between the critical values for the case of global buckling are smaller, and they are almost in the same range. Again, for the case of foams with TD properties, the critical values are predicted to reach the upper range of operating temperature, which is associated with very small values of the core E- and G-moduli. The critical values for the HP foams are higher then those of the P-type foams. For the case of the P foams, the critical temperatures for wrinkling and global buckling are almost identical, and they are in the upper range of the operating temperature for this material. In conclusion, the temperature dependency of polymer foam core materials significantly affects the buckling behavior of sandwich panels with a compliant core. In particular, the

Foam	Buckling-Properties Types	T_{cr}^{o} [C]*	Mode Number (m)	$E_c(T_{cr})$ [MPa]	$G_c(T_{cr})$ [MPa]
HP80	Wr-TI**	356.4	93	63.6	28.4
	Wr-TD	102.2	50	5.4	2.4
	Gl-TI	140.1	1	63.6	28.4
	Gl-TD	95.0	1	13.8	6.2
HP100	Wr-TI	390.8	97	77.0	36.9
	Wr-TD	106.1	51	5.8	2.8
	Gl-TI	144.2	1	77.0	36.9
	Gl-TD	99.8	1	14.6	7.0
HP130	Wr-TI	462.9	106	105.6	44.9
	Wr-TD	155.2	61	12.5	5.3
	Gl-TI	147.1	1	105.6	44.9
	Gl-TD	128.1	1	39.7	16.9
P500	Wr-TI	371.8	95	72.8	38.9
	Wr-TD	71.9	42	2.7	1.4
	Gl-TI	144.4	1	72.8	38.9
	Gl-TD	70.4	1	6.2	3.3
P600	Wr-TI	455.6	105	106.4	49.7
	Wr-TD	68.5	41	2.4	1.1
	Gl-TI	147.9	1	106.4	49.7
	Gl-TD	67.4	1	6.6	3.1
P800	Wr-TI	550.2	116	153.8	68.6
	Wr-TD	69.0	41	2.5	1.1
	Gl-TI	151.2	1	153.8	68.6
	Gl-TD	68.1	1	7.1	3.1

Table 2. Critical temperatures of Divinycell HP and P foams. Legend: Wr – wrinkling mode; Gl – global mode; TI – temperature-independent properties; TD – temperature-dependent properties. *With respect to an unheated panel room temperature (22° C). **Modulus of elasticity and shear modulus at room temperature.

critical temperatures predicted when the temperature dependency is accounted for are always significantly lower than those predicted when the core properties are assumed to be temperature independent, with properties corresponding to room temperature. The reduction is most significant when wrinkling type of buckling occurs, whereas the reduction is less severe for the global buckling mode.

Next, the postbuckling behavior is investigated numerically through the solution of the full nonlinear governing equations under the assumption that a uniform temperature field is applied.

4. Nonlinear governing equations — uniform temperature field

The nonlinear response, for the case of a uniform distribution of the temperature field along the panel length and a linear gradient through its depth (see Figure 1a) is determined. The formulation is based on a set of first-order ordinary differential equations (ODEs) instead of the set of five governing ODEs (see Equations (1) to (4) along with Equations (6) to (9) and Equation (16)). The first-order set consists of fourteen ODEs that are consistent with the fourteen boundary conditions [Frostig 1997]. The transformation of the original ODEs into the first-order has been conducted using well known procedures [Stoer and Bulirsch 1980]. Thus, the nonlinear thermal governing equations read:

(i) For the upper and the lower face sheets ($j = t, b$):

$$\frac{d}{dx} N_{xxj}(x) = (-1)^k \tau(x) b_w - n_j \quad (k = 1 \text{ with } j = t \text{ and } k = 0 \text{ with } j = b),$$

$$\frac{d}{dx} u_{oj}(x) = -\frac{-N_{xxj}(x) - EA_j(x)\alpha_j\left(\frac{1}{2}T_{j_j} + \frac{1}{2}T_{j_b}\right)}{EA_j(x)} - \frac{1}{2} Dw_j(x)^2,$$

$$\frac{d}{dx} V_{xzj}(x) = AA_j b_w - q_j, \quad \text{where } AA_t = -\sigma_{zzt}(x), \ AA_b = \sigma_{zzb}(x),$$

$$\frac{d}{dx} M_{xxj}(x) = V_{xzj}(x) - \frac{1}{2} b_w d_j \tau(x) - N_{xxt}(x)\left(\frac{d}{dx} w_j(x)\right) + m_j(x),$$

$$\frac{d}{dx} w_j(x) = Dw_j(x),$$

$$\frac{d}{dx} Dw_j(x) = -\frac{M_{xxj}(x)}{EI_j} - \frac{\alpha_j(T_{j_b} - T_{j_j})}{d_j}.$$

(ii) For the core:

$$\frac{d}{dx} \tau(x) = D\tau(x) E_{ca} + \frac{-\int_0^c \alpha_c z_c - \frac{1}{2}\frac{E_{c1}(c)\alpha_c c}{E_{c1}(z_c)} - \frac{1}{2}\frac{\alpha_c z_c^2}{c} dz_c T_{c_t} - \int_0^c -\frac{1}{2}\frac{E_{c1}(c)\alpha_c c}{E_{c1}(z_c)} + \frac{1}{2}\frac{\alpha_c z_c^2}{c} dz_c T_{c_b}}{\int_0^c -\frac{1}{E_{c2}(z_c)} + \frac{E_{c1}(c)}{E_{c1}(z_c)E_{c2}(c)} dz_c}, \quad (22)$$

$$\frac{d}{dx} D\tau(x) = \frac{-\frac{\tau(x)}{G_{c1}(c)} + \left(c + \frac{1}{2}d_t - \frac{E_{c1}(c)}{E_{c1z}(c)}\right) Dw_t(x) + \left(\frac{1}{2}d_b + \frac{E_{c1}(c)}{E_{c1z}(c)}\right) Dw_b(x) + u_{ob}(x) - u_{ot}(x)}{\frac{E_{ca}}{E_{c2z}(c)} - \frac{E_{c1}(c)E_{ca}}{E_{c2}(c)E_{c1z}(c)}}, \quad (23)$$

where

$$E_{ca} = \int_0^c \frac{E_c(T_c(x, z_c))}{c} dz_c. \quad (24)$$

The nonlinear response is determined numerically using trapezoid or mid-point methods with Richardson extrapolation or deferred corrections (see [Ascher and Petzold 1998]), as implemented in Maple.
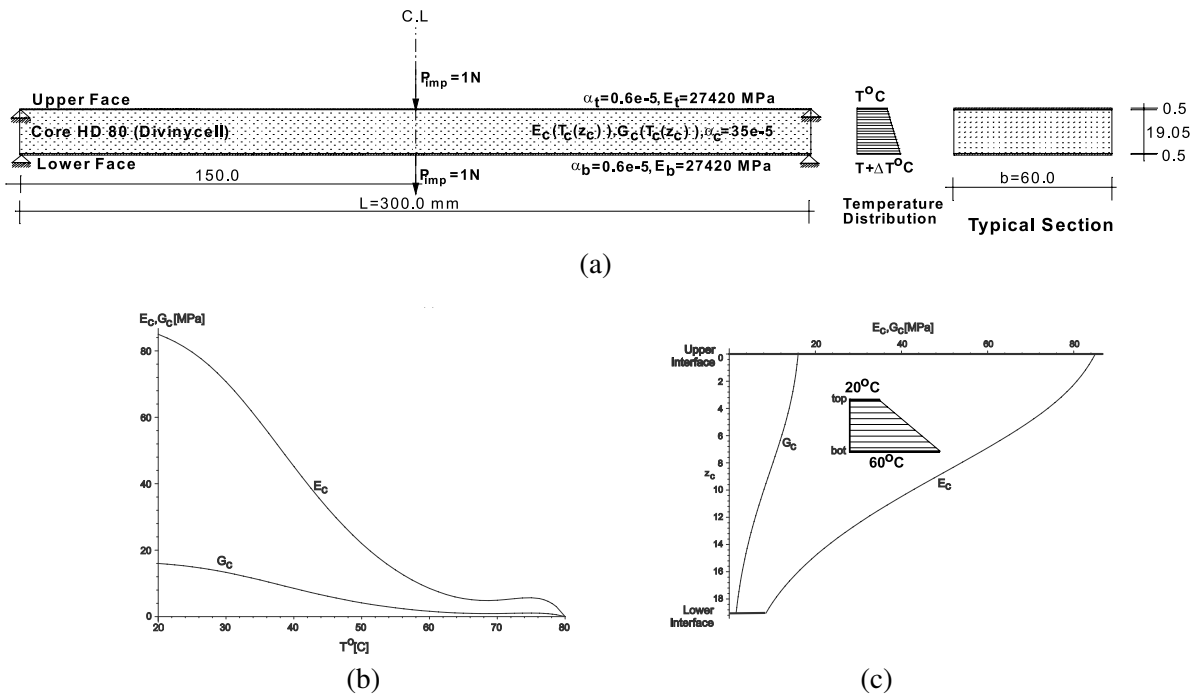
(a)

(b)   (c)

Figure 3. Geometry and temperature-dependent properties of the core and its distribution: (a) geometry and mechanical properties; (b) temperature dependence of elastic and shear moduli of core; (c) distribution of moduli through depth of core for a thermal gradient of 40° C

5. Nonlinear thermomechanical response — numerical study

The numerical study consists of two parts. In the first part the postbuckling response of sandwich panels due to thermally induced deformation associated with a thermal gradient through the core depth is investigated. The second part of the study investigates the nonlinear interaction response when a sandwich panel is loaded simultaneously by an external mechanical load and thermal load with a gradient through the core depth.

5.1. *Postbuckling response.* The postbuckling response plays a major role in the safe design of sandwich panels. It defines whether the buckling loads may be exceeded based on the stability of the sandwich assembly. In general, the postbuckling response can be characterized as belonging to one of the following types: beam, plate or shell form. The plate type response is considered as stable, since any additional deformation is associated by a load increase, while the beam and shell types are unstable since any additional displacement is associated with an unchanged or a reduced load. The postbuckling response of a sandwich panel may fall into all three categories (see [Sokolinsky and Frostig 2000]) depending on the geometry, loading scheme, mechanical properties and boundary conditions.

The study investigates the effects of a thermal gradient through the core depth on the postbuckling response, assuming TD and TI elastic properties. It is assumed that the distribution of the temperatures

through the thickness of each face sheet is uniform, and the difference in temperatures, ΔT, between the lower and upper face sheets is changing from 0° to 40° C (see Figure 3a, where $T_b = T_t + \Delta T$). The temperature at the upper face sheet is increased from 20° C until the lower face sheet reaches a temperature of 79° C.

The nonlinear response examines a typical sandwich panel with face sheets made of Kevlar composite faces and a HD 80 foam core from DIAB. The geometry of the panel and the temperature distribution through the depth of the panel appear in Figure 3a. The panel is pin supported at the edges of the face sheets, which are restrained longitudinally. The temperature distribution is uniform through the length of the panel. The moduli of the core are temperature-dependent, and the $E_c(T)$, $G_c(T)$ versus temperature (T) plots appear in Figure 3b, in the temperature range 20–80° C, based on the data in [Diab Group 2003].

The fitted curve moduli are based on data from [Diab Group 2003] and Figure 3b. The variations of the E- and G-moduli through the depth of the core for a thermal gradient of $\Delta T = 40^o$ C ($T_t = 20^o$ C and $T_b = 40^o$ C) are significant (see Figure 3c).

A global buckling mode has been detected for this case, within the range of the operating temperatures of the foam, and in order to initiate a global buckling mode an imperfection in the form of two very small concentrated loads of 1N have been applied in the same direction to the two face sheets at mid-span, see Figure 3a.

The results corresponding to global buckling of the sandwich panel heated by a uniform temperature field in the longitudinal and the vertical directions appear in Figure 4. The results along the half length of the panel are presented at five different temperature levels. The vertical displacements appear in Figure 4a and reveal that the faces move in opposite directions (upwards and downwards) in the vicinity of the supports as a result of the expansion of the core in the vertical direction. The displacements at mid-span at a temperature of 78° C reach very large values, as compared to those values reached at lower temperatures, due to the loss of the rigidity of the core at this elevated temperature level. The bending moments that are quite small (see Figure 4b) yield localized effects in the vicinity of the support as a result of the inability of the core to expand vertically due to the thermal strains. In addition, bending moments are induced around mid-span due to the small imperfection loads. The in-plane stress results, which are mainly caused by the longitudinal restraints of the supports, appear in Figure 4c. These forces are not constant, due to the existence of shear stresses at the face–core interfaces. Finally, the vertical interfacial stresses appear in Figure 4d, for which it is observed that large localized effects occur in the vicinity of the supports as a result of restraining the expansion of the core in the vertical direction. Small vertical normal stresses occur around mid-span due to the imperfection loads.

The equilibrium curves appear for all temperature gradients in Figure 5, which also includes the cases of TD and TI core properties. The equilibrium curves have been determined using a parametric continuation procedure up to the temperature level when either the solution does not converge, or the upper limit of the range of the operating temperatures (20 to 80° C) has been reached. Hence, there is no case where the E- and G-moduli reaches the value of zero within the core depth. The temperature versus the maximum vertical displacements at the upper and the lower face sheets, assuming a core either with or without temperature dependent properties, appears in Figure 5a. The temperature independent core with room-temperature properties yields a linear curve, almost constant for all gradients, which indicates
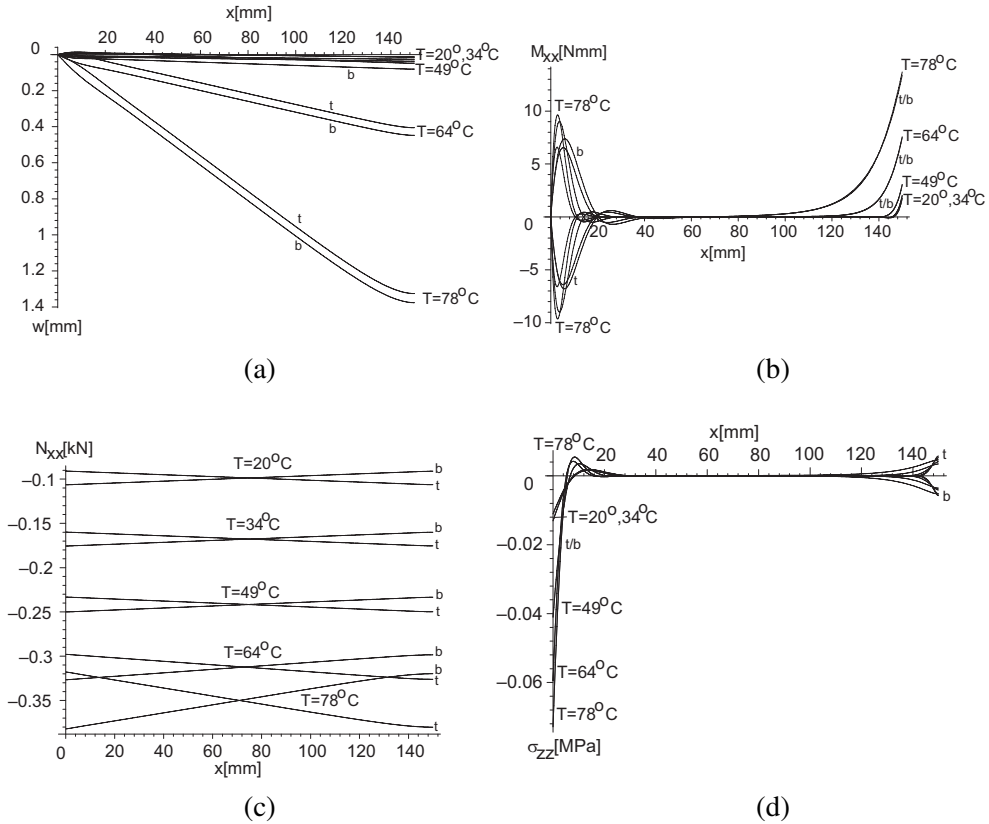
Figure 4. Postbuckling results along the length of a restrained sandwich panel with a zero thermal gradient at various temperatures: (a) vertical displacements, (b) bending moments, (c) in-plane stress resultants, (d) interfacial vertical normal stresses at interfaces. Legend: —— t upper face/ interface; - - - - b lower face/ interface.

that the panel does not buckle within this range of temperatures (denoted by TI). The results reveal also that in the case of *zero* thermal gradient (a uniform distribution in the vertical direction) the behavior is stable up to 77° C, and beyond this temperature the sandwich panel collapses as a result of the very low rigidity of the core. For the case of a thermal gradient of $\Delta T = 10^o$ C, the equilibrium curves exhibit a nonlinear stable response. A nonlinear behavior with smaller deformations occurs for all gradients. The temperature versus the extreme compressive values of the vertical interfacial stresses appear in Figure 5b for cores with and without temperature dependent properties. For the temperature independent case at $\Delta T = 0^o$ C (uniform) and $\Delta T = 40^o$ C, linear responses occur, that is, the peak vertical interfacial stresses (compressive) increase with increasing temperature as a result of the large expansion of the core in the vertical direction (restrained by the fixity of the supports in the vertical direction). The curves obtained for the temperature dependent cores exhibit a nonlinear pattern where the maximum compressive stress occurs around 30° C for all cases. The maximum compressive stresses occur at the support, as a result of the restraint of the expansion of the core in the vertical direction, along with the relatively undegraded core properties (around 30° C) and the minor influence of the global buckling mode.
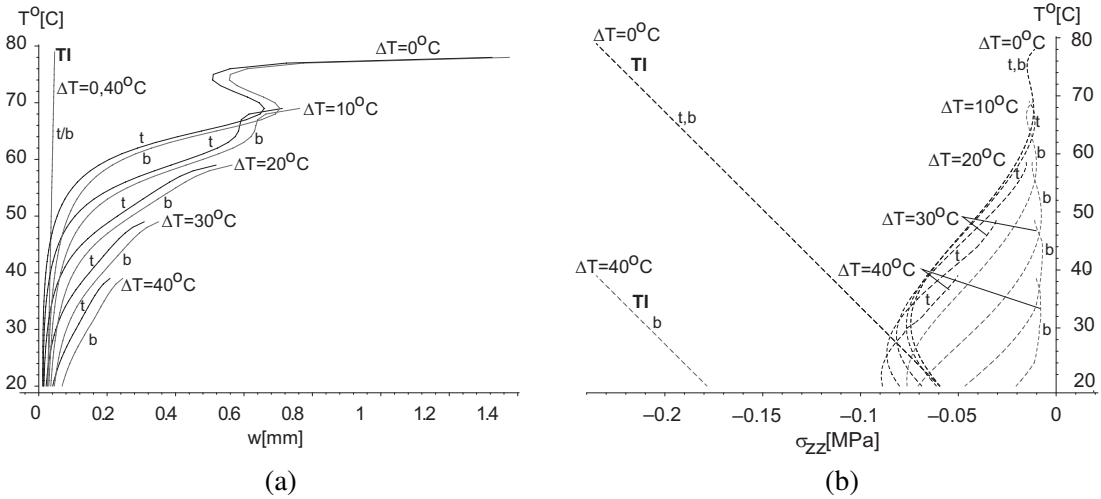
Figure 5. Temperature equilibrium curves of maximum values for a restrained sandwich panel subjected to various thermal gradients: (a) maximum vertical displacements of face sheets, (b) maximum compressive interfacial vertical normal stresses at interfaces. Legend: ——— t upper face or interface; - - - - b lower face or interface.

5.2. *Interaction of mechanical loads and thermally induced deformations.* The nonlinear thermome-chanical response of restrained and unrestrained sandwich panels loaded by a prescribed mechanical load and a changing thermal gradient is studied. In addition, the study examines the effects on the response of elevated temperature in the imposed thermal gradient when applied either to the tensile (Ten) face sheet or to the compressive (Com) face sheet. Notice that a linear response occurs when the loads are applied separately as well as when the two loads are applied simultaneously, and the core properties are TI.

The investigated sandwich panel consists of two face sheets made of Kevlar composite laminates and a Divinycell core made of HD-80 foam. The layout, dimensions, mechanical properties and loadings appear in Figure 6a. The panel is loaded in a three-points bending scheme, where the load is applied at the upper face sheet and the panel is supported only at its lower face sheet, while the edges of its core and upper face are free of force tractions. The fixity of the panel is achieved by imposing longitudinal restraints on the edges of the face sheets (see dotted supports in Figure 6a). The thermal gradient is imposed only within the core with two different variants (see temperature distribution in Figure 6a). In the first variant the highest temperature is imposed at the lower tensile face sheet (Ten), while in the second variant the highest temperature is imposed at the upper compressed face sheet (Com). The temperature-dependent properties of the core are the same as in the previous case. See Figure 3b and Figure 3c for temperature dependency of the E- and G-moduli and their distribution through the core depth for a gradient of 40° C. The solution procedure uses a parametric continuation approach with the temperature T as the parameter. The procedure halts when the solution does not converge or when it violates the assumption of large displacements and moderate rotations, which in this study occurs when the maximum displacement approaches a value of $L/10$. The results are also limited to a temperature of 79° C, which represents the upper limit of the range of operating temperatures for this particular temperature-dependent DIAB core (HD80).
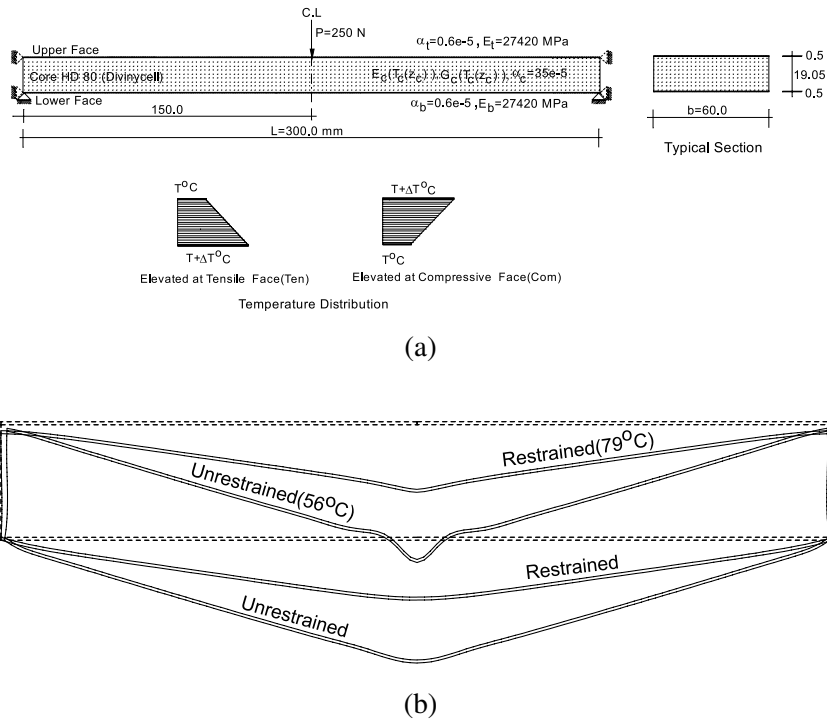
(a)

(b)

Figure 6. Geometry and deformed shapes of sandwich panel loaded by a mechanical load and thermally induced deformations with a zero thermal gradient: (a) geometry of unrestrained and restrained panels; (b) deformed shape of an unrestrained at $T = 56^o$ C and a restrained panel at $T = 79^o$ C.

The deformed shapes of a sandwich panel which is considered to be either longitudinally restrained or nonrestrained at uniform (zero gradient through the core depth) temperatures of 79° C and 56° C, respectively, appear in Figure 6b. The displacements patterns for the two cases are very different, and it is seen that the displacements for the case of the unrestrained sandwich panel are much larger than for the restrained case. Notice that the indentation zone in the vicinity of the load is significant for the unrestrained deformation pattern, whereas it is almost invisible for the restrained case. If the core material properties are temperature independent and stiffness properties corresponding to room-temperature are used, the predicted deformations are much smaller (see Figure 8a). Moreover, notice that the upper face sheet in the two cases has settled as a result of the unsupported edge.

The results obtained for an unrestrained sandwich panel with a zero gradient through the core depth appear in Figure 7 at five different temperature levels; 20° C, 29° C, 39° C, 49° C and 56° C. The vertical displacements appear in Figure 7a where it is observed that an indentation occurs at mid-span for all temperature levels. Moreover, it is seen that the magnitude of the indentation increases with increasing temperature as a result of the degradation of the mechanical properties of the core. The mid-span displacement at the highest temperature (56° C) is about 2.5 times larger than the mid-span displacement corresponding to the temperature immediately below (49° C) as a result of the loss of stability (see Figure
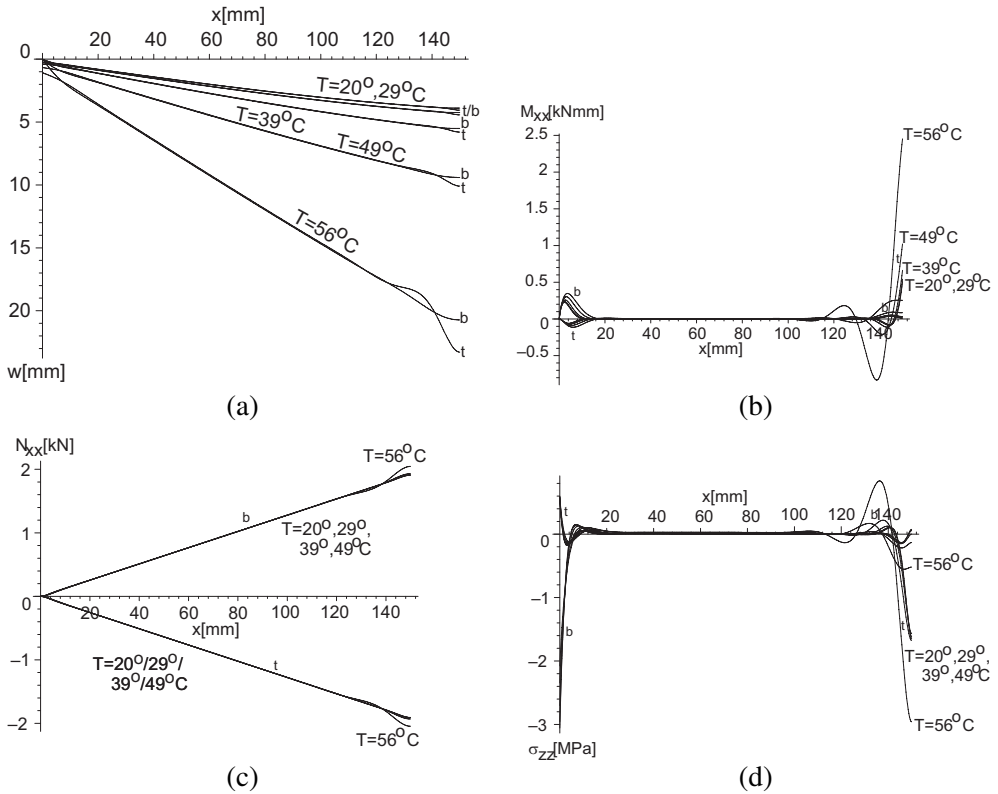
Figure 7. Nonlinear response along sandwich panel loaded simultaneously by a mechanical load and thermally induced deformations with a zero thermal gradient at various temperatures: (a) vertical displacements, (b) bending moments, (c) in-plane stress resultants, (d) interfacial vertical normal stresses at interfaces. Legend: —— t upper face/ interface; - - - - b lower face/interface.

8a). From the bending moment diagrams (see Figure 7b) it is observed that significant bending moments are present and reach very high values at higher temperatures. The in-plane stress resultants of the face sheets appear in Figure 7c, where it is seen that fluctuations occur around mid-span only at high temperatures as a result of the large vertical displacements in this area. Notice that the in-plane stress resultants are nearly unaffected by the thermal loading, since the structure is statically determined and the overall bending moment corresponds to the three point bending load case. The mid-span fluctuations seen at the highest temperature (56° C) are due to the reduced core height, which is caused by the large vertical displacements in this vicinity (see Figure 7a). Finally, the interfacial vertical normal stresses appear in Figure 7d. From Figure 7d it is seen that very high stresses are induced in the vicinities of the support and the mid-span load at high temperatures as a result of the large displacements and the reduced rigidity of the core.

In Figures 8 and 9, the equilibrium curves are presented for both types of sandwich panels, those with and those without longitudinal restraints, and for all thermal gradients. In addition, three different
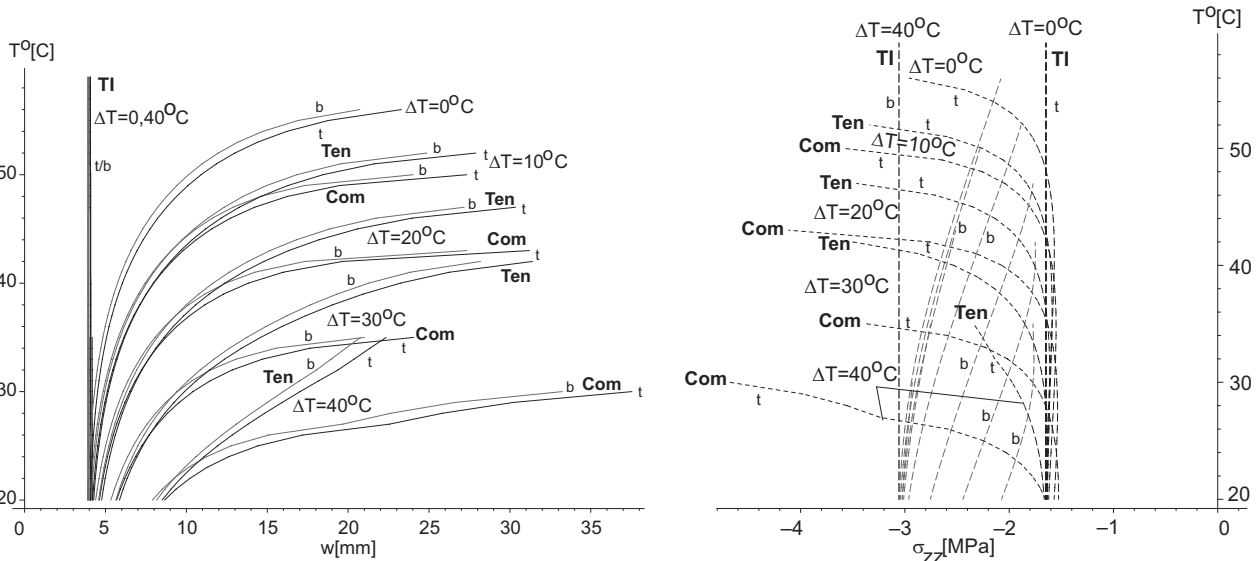
Figure 8. Temperature equilibrium curves of maximum displacements and vertical normal stresses versus temperature for an *unrestrained* sandwich panel loaded with mechanical and thermal loads simultaneously, with temperature-independent and temperature-dependent properties at various thermal gradients, and where the elevated temperatures are imposed either on the tensile (Ten) or the compressed (Com) face sheet: (a) maximum vertical displacements, (b) maximum compressive interfacial vertical normal stresses at interfaces. Legend: ——— t upper face or interface; - - - - - -b lower face or interface.

cases of thermal effects are presented. The first case represents a sandwich panel with TI core properties. The other two cases examine a core with temperature-dependent properties, one case where elevated temperatures are imposed at the tensile face sheets (Ten), and another where elevated temperatures are imposed at the face sheets loaded in compression (Com).

The equilibrium curves for the unrestrained sandwich panel appear in Figure 8. The equilibrium curves of temperature versus maximum vertical displacement appear in Figure 8a. For the TI case it is seen that a thermal gradient exerts a minor effect on the response, which remains linear through the entire range of working temperatures. For the TD cases it is seen that unstable behavior with very large displacements are seen for all thermal gradients at temperatures that lie well below the upper limit of the range of operating temperatures. For the zero thermal gradient case, denoted by $\Delta T = 0^o$ C, the instability starts around 55° C. Beyond 56° C the panel reaches extremely large displacements. The results reveal that when the tensile face sheet is warmer than the bottom face, loss of stability always occurs at a higher temperature than when the compressed face sheet is warmer. This difference is especially significant at a thermal gradient of 40° C. Notice that at this gradient the case with a warmer tensile face sheet exhibits a stable nonlinear behavior, while the case where the compressed face sheet is warmer yields an unstable pattern with the probable existence of a limit point at a very low temperature. The same trends are observed for the maximum compressive interfacial vertical normal stresses (see Figure 8b). In all cases,
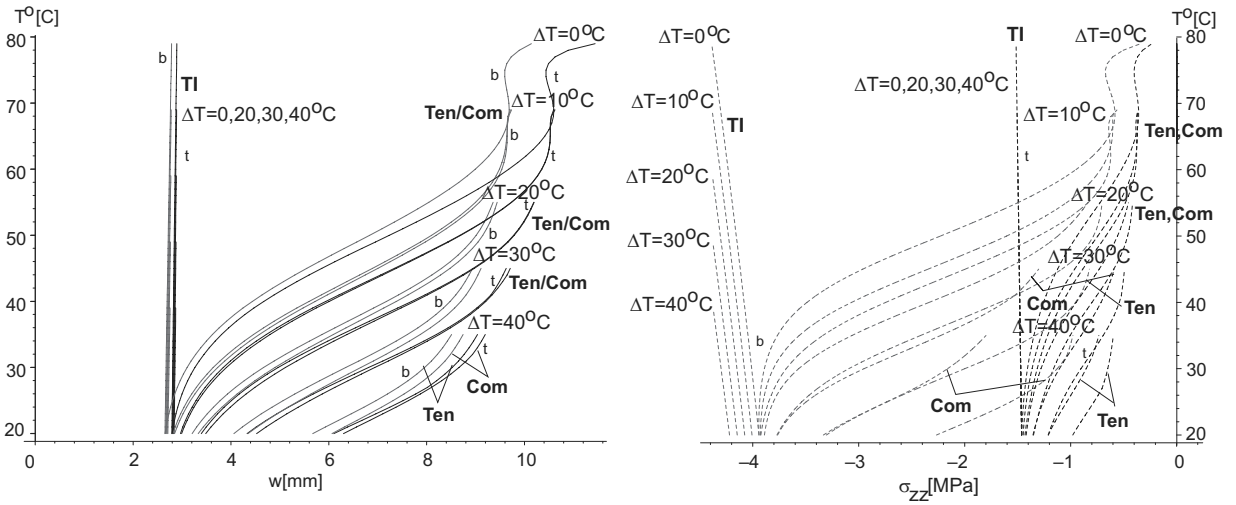
Figure 9. Temperature equilibrium curves of maximum displacements and vertical normal stresses versus temperature for a *restrained* sandwich panel loaded with mechanical and thermal loads simultaneously, with temperature-independent and temperature-dependent properties at various thermal gradients and where the elevated temperatures are imposed either on the tensile (Ten) or the compressed (Com) face sheet: (a) maximum vertical displacements of face sheets; (b) maximum compressive interfacial vertical normal stresses at interfaces. Legend: ——— t upper face or interface; - - - - b lower face or interface.

larger compressed stresses are observed when the compressed face sheet is warmer. They always reach very high values, which may exceed the allowable compressive normal stresses (compressive strengths at the relevant temperatures) of the core.

The equilibrium curves for the restrained sandwich panel case appear in Figure 9. The curves of temperature versus maximum values of the vertical face sheet displacements appear in Figure 9a. Again, the TI core yields a linear response, which is associated with larger displacement with increasing thermal gradient, but the peak displacements are still quite small. In contrast to this, the TD cases behave in a stable nonlinear manner, and in all cases the upper limit of the temperature range has been reached. The zero thermal gradient case is the most sensitive one. It consists of a stable curve up to 77° C, and above this temperature the equilibrium curve shows signs of loss of stability similar to the postbuckling case shown in Figure 5a. Generally, in this case it matters little if the compressed face sheet is warmer than the tensile face sheet, and vice versa. The same trends are observed for the maximum compressive interfacial vertical normal stresses (see Figure 9b). Here, notice that in all cases the larger compressive stress occurs at the supports and at the lower temperatures as a result of the fixity of the supports and the high resistance (rigidity) of the core. As the temperatures are raised this resistance reduces due to the degradation of the core material, and much smaller interfacial stresses are induced. This is exactly opposite to the case where the core is assumed to have TI properties. For the TI core case the resistance

of the core is unaffected by increased temperatures, and therefore the higher thermal strains cause higher stresses with a linear behavior.

6. Summary and conclusions

The nonlinear thermal behavior, buckling and postbuckling of a sandwich panel with a compliant core that has temperature-dependent properties is presented. The analysis considers the thermal strains of the core in the vertical direction along with the effects of the vertical flexibility of the core using variational principles and the HSAPT approach. The temperature-dependent properties of the core, along with a thermal gradient, yields stiffness coordinates dependent properties. The stress and displacement fields of the core with such nonuniform properties have been solved analytically.

The buckling analysis follows the perturbation technique. It yields a nonlinear set of algebraic equations which are solved numerically for the wrinkling and the global buckling critical temperatures, assuming a uniform temperature field, simple support conditions and temperature-dependent core properties.

The nonlinear response is determined through a numerical solution of a set of coupled first-order nonlinear ordinary differential equations. The parametric continuation procedure, using the temperature at one of the face sheet as a parameter, has been used to determine the equilibrium curves.

The numerical study includes the responses due to buckling, postbuckling and interactions between mechanical loads and thermal ones. The buckling study examines various foam cores including Rohacell foam from Rohm GmbH & Co. KG and the P and HP Divinycell foams from DIAB. A comparison between the critical wrinkling and global buckling temperatures for a core with TI mechanical properties (room-temperature properties assumed) and a core with TD mechanical properties has been conducted. In all cases the analyses predict a significant reduction of the critical wrinkling temperature of the TD core panels, along with changes in the number of half-waves in the buckling pattern, in comparison with panels with TI cores. The changes in the critical temperatures corresponding to the global buckling mode are much smaller (10 to 30%). In all cases, for a particular sandwich panel configuration, the critical temperatures are predicted to be in the upper part of the feasible range of working temperatures.

The numerical study of the nonlinear response consists of two parts. In the first part a postbuckling response of a panel subjected to a thermal gradient loading with fixed support is examined. The second part examines the effect of rising temperatures imposed simultaneously with a prescribed mechanical load, on either the tensile or the compressed face sheets. The effect on the mechanical response of the sandwich panel with and without restrained supports is measured.

The postbuckling study reveals that for the case of a uniform temperature field the nonlinear response is stable as a result of the fixity of the supports in the longitudinal direction, as long as the temperatures are below the upper limit of the working temperature range. As the temperature approach this value, the panel looses its stability with very large displacements and high stresses due to the very low elastic moduli of the core at elevated temperatures. For all other cases, with a gradient through the depth of the core, the response is stable within the feasible working temperature range.

The interaction between a mechanical load and rising temperature at the tensile and compressive face sheets has been studied for restrained and unrestrained sandwich panels with and without a TI core. The results reveal that the response, for an unrestrained sandwich with a temperature-independent core, remains linear and constant through the entire range of working temperatures. In contrast to this, for the

case of a temperature-dependent core, the response is nonlinear and loss of stability occurs far below the upper limit of the operational temperature range. The case where the elevated temperature is imposed on the compressed face is even more severe, and loss of stability occurs at temperatures below those predicted for the case where the tensile face sheet is warmer. For sandwich panels with fixed boundary conditions (full restraint) the nonlinear response generally is of a stable type.

The interaction between mechanical and a thermally induced deformation loads is highly relevant and likely to occur under practical service conditions. This is especially the case for unrestrained sandwich panels with temperature-dependent core properties (as is always the case for polymer foam core materials), and such interactions may seriously affect structural reliability and safety. Hence, it is important to assess these effects for a reliable design of sandwich panels/structures. This implies that a nonlinear analysis procedure, which accounts for the compliant temperature-dependent core properties and the interaction between the mechanical loads and the loads due to thermally induced deformations, must be adopted.

Acknowledgements

References

[Allen 1969] H. G. Allen, *Analysis and design of structural sandwich panels*, Pergamon Press, Oxford, 1969.

[Ascher and Petzold 1998] U. Ascher and L. Petzold, *Computer methods for ordinary differential equations and differential-algebraic equations*, SIAM, Philadelphia, 1998.

[Birman 2005] V. Birman, "Thermally induced bending and wrinkling in large aspect ratio sandwich panels", *Compos. Part A Appl. S.* **36**:10 (2005), 1412–1420.

[Birman et al. 2006] V. Birman, G. A. Kardomateas, G. J. Simitses, and R. Li, "Response of a sandwich panel subject to fire or elevated temperature on one of the surfaces", *Compos. Part A Appl. S.* **37**:7 (2006), 981–988.

[Chen and Chen 1989] L. W. Chen and L. Y. Chen, "Thermal buckling behavior of laminated composite plates with temperature-dependent properties", *Compos. Struct.* **13**:4 (1989), 275–287.

[Chen and Chen 1991] L. W. Chen and L. Y. Chen, "Thermal postbuckling behaviors of laminated composite plates with temperature-dependent properties", *Compos. Struct.* **19**:3 (1991), 267–283.

[Diab Group 2003] "Data sheet HD grade", Technical report, Diab Group, 2003.

[Diab Group 2005] Diab Group, "P and HP-core — test protocol", 2005. Private communication.

[Frostig 1997] Y. Frostig, "Hygothermal (environmental) effects in high-order bending of sandwich beams with a flexible core and a discontinuous skin", *Compos. Struct.* **37**:2 (1997), 205–221.

[Frostig 1998] Y. Frostig, "Buckling of sandwich panels with a flexible core-high-order theory", *Int. J. Solids Struct.* **35**:3-4 (1998), 183–204.

[Frostig and Baruch 1993] Y. Frostig and M. Baruch, "High-order buckling analysis of sandwich beams with transversely flexible core", *J. Eng. Mech. ASCE* **119**:3 (1993), 476–495.

[Frostig and Thomsen 2007a] Y. Frostig and O. T. Thomsen, "Non-linear thermal response of sandwich panels with a flexible core and temperature dependent mechanical properties", 2007. In press.

[Frostig and Thomsen 2007b] Y. Frostig and O. T. Thomsen, "Thermal buckling and post-buckling of sandwich panels with a transversely flexible core", 2007. Submitted.

[Frostig et al. 2005] Y. Frostig, O. T. Thomsen, and I. Sheinman, "On the non-linear high-order theory of unidirectional sandwich panels with a transversely flexible core", *Int. J. Solids Struct.* **42**:5–6 (2005), 1443–1463.

[Gu and Asaro 2005] P. Gu and R. J. Asaro, "Structural buckling of polymer matrix composites due to reduced stiffness from fire damage", *Compos. Struct.* **69**:1 (2005), 65–75.

[Huang and Kardomateas 2002] H. Y. Huang and G. A. Kardomateas, "Buckling and initial postbuckling behavior of sandwich beams including transverse shear", *AIAA J.* **40**:11 (2002), 2331–2335.

[Kant and S. 2000] T. Kant and B. C. S., "Thermal buckling analysis of skew fibre-reinforced composite and sandwich plates using shear deformable finite element models", *Compos. Struct.* **49**:1 (2000), 77–85.

[Kapuria and Achary 2004] S. Kapuria and G. G. S. Achary, "An efficient higher-order zigzag theory for laminated plates subjected to thermal loading", *Int. J. Solids Struct.* **41**:16-17 (2004), 4661–4684.

[Kardomateas and Huang 2003] G. A. Kardomateas and H. Huang, "The initial post-buckling behavior of face-sheet delaminations in sandwich composites", *J. Appl. Mech.* (*Trans. ASME*) **70**:2 (2003), 191–199.

[Ko 1994] W. L. Ko, "Mechanical and thermal buckling analysis of rectangular sandwich panels under different edge conditions", Technical report TM-4585, National Aeronautics and Space Administration, 1994, Available at http://ntrs.nasa.gov/search.jsp?R=952948&id=2&qs=Ne%3D20%26N%3D4294826073%2% B53.

[Liew et al. 2004] K. M. Liew, J. Yang, and S. Kitipornchai, "Thermal post-buckling of laminated plates comprising functionally graded materials with temperature-dependent properties", *J. Appl. Mech.* (*Trans. ASME*) **71**:6 (2004), 839–850.

[Liu et al. 2006] L. Liu, G. A. Kardomateas, V. Birman, J. W. Holmes, and G. J. Simitses, "Thermal buckling of a heat-exposed, axially restrained composite column", *Compos. Part A Appl. S.* **37**:7 (2006), 972–980.

[Matsunaga 2005] H. Matsunaga, "Thermal buckling of cross-ply laminated composite and sandwich plates according to a global higher-order deformation theory", *Compos. Struct.* **68**:4 (2005), 439–454.

[Mindlin 1951] R. D. Mindlin, "Influence of transverse shear deformation on the bending of classical plates", *J. Appl. Mech.* (*Trans. ASME*) **8** (1951), 18–31.

[Najafizadeh and Heydari 2004] M. M. Najafizadeh and H. R. Heydari, "Thermal buckling of functionally graded circular plates based on higher-order shear deformation plate theory", *Eur. J. Mech. A Solids* **23**:6 (2004), 1085–1100.

[Plantema 1966] F. J. Plantema, *Sandwich construction: the bending and buckling of sandwich beams, plates, and shells*, Wiley, New York, 1966.

[Reddy 1984] J. N. Reddy, *Energy and variational methods in applied mechanics: with an introduction to the finite element method*, John Wiley, New York, 1984.

[Rohacell 2004] Degussa, WF foam data sheets, 2004. Available from www.rohacell.com through the link Site Map.

[Shiau and Kuo 2004] L. C. Shiau and S. Y. Kuo, "Thermal postbuckling behavior of composite sandwich plates", *J. Eng. Mech. ASCE* **130**:10 (2004), 1160–1167.

[Simitses 1976] G. J. Simitses, *An introduction to the elastic stability of structures*, Prentice-Hall, Englewood Cliffs, NJ, 1976.

[Sokolinsky and Frostig 2000] V. Sokolinsky and Y. Frostig, "Branching behavior in the nonlinear response of sandwich panels with a transversely flexible core", *Int. J. Solids Struct.* **37**:40 (2000), 5745–5772.

[Stoer and Bulirsch 1980] J. Stoer and R. Bulirsch, *Introduction to numerical analysis*, Springer, New York, 1980.

[Tessler et al. 2001] A. Tessler, M. S. Annett, and G. Gendron, "A {1, 2}-order plate theory accounting for three-dimensional thermoelastic deformations in thick composite and sandwich laminates", *Compos. Struct.* **52**:1 (2001), 67–84.

[Vinson 1999] J. R. Vinson, *The behavior of sandwich structures of isotropic and composite materials*, Technomic Publishing, Lancaster, PA, 1999.

[Zenkert 1995] D. Zenkert, *An introduction to sandwich construction*, Engineering Materials Advisory Services, West Midlands, UK, 1995.

YEOSHUA FROSTIG: cvrfros@techunix.technion.ac.il
Faculty of Civil Engineering, Technion — Israel Institute of Technology, Haifa 32000, Israel

OLE THYBO THOMSEN: ott@ime.aau.dk
Department of Mechanical Engineering, Aalborg University, Pontoppidanstraede 101, DK-9220 Aalborg, Denmark